Molecular Therapy
Nucleic Acids
Original Article

Antithrombotic Effect of shRNA Target *F12* Mediated by Adeno-Associated Virus

Fanfan Li,[1] Xiao Yang,[1] Jie Liu,[1] Kuangyi Shu,[1] Chenfang Shen,[1] Tao Chen,[1] Wei Yang,[1] Shanshan Li,[1] Xiaoou Wang,[1] and Minghua Jiang[1]

[1]The Second Affiliated Hospital and Yuying Children's Hospital of Wenzhou Medical University, Wenzhou, Zhejiang Province 325000, China

Coagulation factor XII (FXII) plays a crucial role in thrombosis. Moreover, deficiencies in FXII are not associated with excessive bleeding, and its depletion exhibits satisfactory protective effect on thrombus formation. Several strategies targeting FXII have been applied to inhibit thrombosis formation. In this study, C57BL/6 mice were injected with adeno-associated virus (AAV) to identify the role of short hairpin RNA (shRNA) in thrombosis. Differences in liver FXII, coagulation function, and thrombus formation were detected. The potential side effects of FXII were then evaluated through analysis of tail bleeding, biochemical indices, and pathological sections. Results showed that shRNAs, especially shRNA2, carried by AAV, effectively reduced the expression of FXII. Furthermore, only shRNA2 demonstrated an anti-thrombosis effect on multiple models without hemorrhage and side effects. Hence the novel approach of AAV-based shRNA is specific and safe for inhibiting FXII and thrombosis.

INTRODUCTION

The extrinsic pathway initiates thrombin formation at injured regions, whereas the intrinsic pathway mediates continuous thrombin production and fibrin clot generation to stabilize a thrombus. Factor XII (FXII) is the initiator of the intrinsic pathway and is analogous to fibrinolytic proteins; FXII can be activated to form FXIIa via contact with negatively charged substances, such as polyphosphates,[1] nucleic acids,[2,3] protein aggregates,[4] and collagen.[5] Once activated, FXIIa immediately catalyzes FXII and prekallikrein (PK) to trigger the intrinsic pathway and the kallikrein kinin system (KKS),[6] which are closely related to coagulation and inflammatory responses.[7]

FXII can effectively start the intrinsic coagulation pathway but is nonessential for hemostasis.[8] Previous research showed that FXII deficiency in humans and animals often occurs asymptomatically, and the depletion of plasma FXII can protect animals from thrombosis in various models.[9] Therefore, new methods have been applied to inhibit FXII and prevent thrombus formation. For example, antisense oligonucleotide,[10,11] RNA aptamer,[12] and antibodies[13] can efficiently suppress FXII expression and thrombosis *in vitro* or *in vivo*. However, none of these approaches can maintain a stable inhibitory effect without repeated injections.[14]

RNAi has been widely used to silence genes by regulating the expression of specific mRNA. Compared with chemically synthesized siRNA, vector-based short hairpin RNAs (shRNAs) can be expressed intracellularly and effectively trigger long-lasting RNAi.[15] At present, adeno-associated virus (AAV) has become the most widely applied vector to animal research and liver gene therapy because of the advantageous biological property of infecting a wide range of host cell types, such as liver.[15]

This study aims to determine whether AAV-based shRNAs targeting FXII (AAV-shRNAs) exert considerable antithrombotic effect *in vivo*. Accordingly, our study demonstrated that FXII could be significantly reduced, and that selective knockdown of FXII prevented thrombus formation in arterial and venous thrombosis models without additional histologic lesion and hemorrhage.

RESULTS

Transfection Efficiency of AAV in Mouse Livers

Previous studies proved that utilizing an adeno-associated virus serotype 8 (AAV8) vector can remarkably improve infection efficiency in mouse livers. Thus, we constructed an AAV8 vector expressing either *F12*-shRNAs (shRNA1 and shRNA2) or negative control (NC) shRNA (nc-shRNA) from a U6 promoter and ZsGreen reporter (Figure S1). At 21 days after injection, the mouse livers were used to examine ZsGreen signals. Figure 1A shows that AAV8-treated livers exhibited highly efficient expression of ZsGreen, thereby indicating the superior transfection efficiency of AAV8.

Reduction of Hepatic FXII in mRNA and Protein Levels

In order to identify the interference effects of shRNAs, the livers were used to detect *F12* mRNA and protein levels. Quantitative real-time PCR data analyses revealed that the mRNA expression in the shRNA1 and shRNA2 groups decreased to 48% and 17% of the value in PBS-treated mice. No difference was found between nc-shRNA-treated and PBS-treated mice (Figure 1B), thereby confirming that the knockdown of *F12* was caused by shRNAs and not AAV8. In addition, we simultaneously tested the change of *F7*, which was important in

Received 12 July 2018; accepted 28 February 2019;
https://doi.org/10.1016/j.omtn.2019.02.026.

Correspondence: Minghua Jiang, The Second Affiliated Hospital and Yuying Children's Hospital of Wenzhou Medical University, 109 Xueyuan West Road, Wenzhou, Zhejiang Province 325000, China.
E-mail: minghua93@126.com

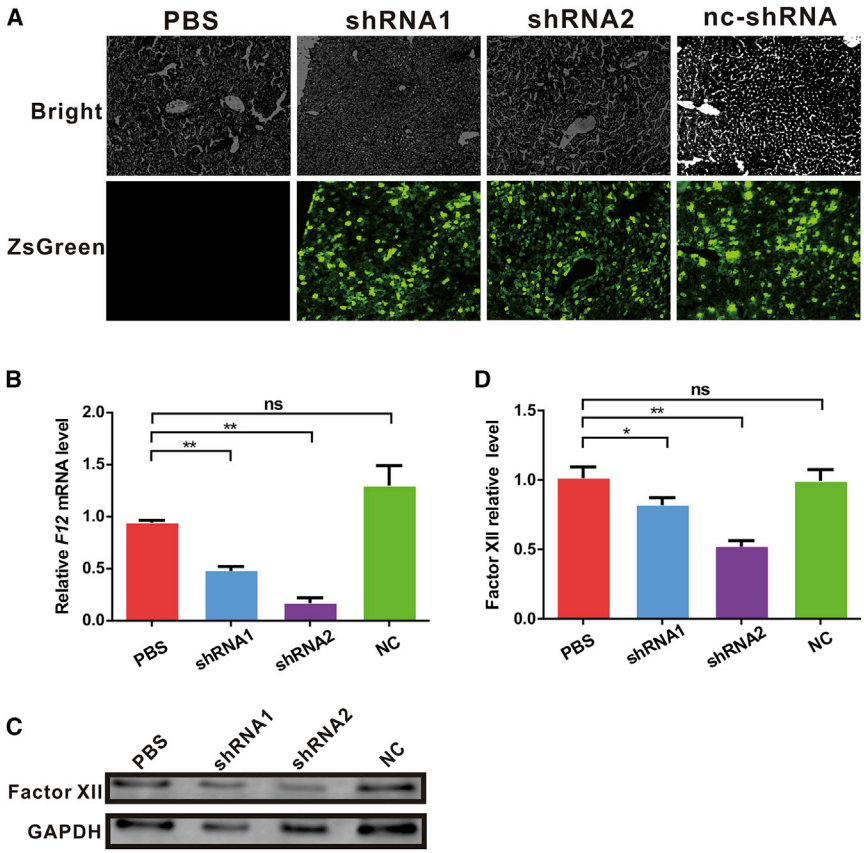

Figure 1. Transfection Efficiency and Knockdown of *F12* in Livers

(A) Images of mouse livers for detecting ZsGreen signals. (B) Mice were collected for quantification of hepatic FXII mRNA levels. (C) Protein levels of hepatic FXII were detected by immunoblot analysis. (D) FXII relative protein levels were quantified by densitometry. Error bars are SD (n = 3); $^{ns}p > 0.05$, $^{*}p < 0.05$, $^{**}p < 0.01$.

thrombosis and bleeding. The results presented that shRNAs did not alter the *F7* (Figure S2A). We then determined whether the protein has the same changes in shRNAs-treated mice. Figures 1C and 1D show that the protein expression in the shRNA1 and shRNA2 groups were reduced by 18% and 48% compared with that in PBS-treated mice. Hence shRNAs could significantly decrease FXII, especially shRNA2.

Comparison of Coagulation Function in Plasmas

To determine the influences of the coagulation function, we collected mouse plasmas for further experiments. The western blot results showed remarkable difference in FXII between the shRNA2-treated group (declined to 40%) and the shRNA1-treated group (reduced to 72%) (Figures 2A and 2B). These results are consistent with FXII activity in the shRNA1, shRNA2, nc-shRNA, and PBS groups, with values of 0.48 ± 0.12, 0.22 ± 0.07, 0.85 ± 0.19, and 1.00 ± 0.19, respectively (Figure 2C). As shown in Figure 2D, the *ex vivo* activated partial thromboplastin time (APTT) in the shRNA1 group remained the same level (22.13 ± 3.70 s) as that of the control, inconsistent with the results of plasma FXII antigen and activity. Moreover, shRNA2-treated mice (36.30 ± 1.84 s) displayed significant prolonged APTT compared with that in the nc-shRNA (20.87 ± 1.82 s) and PBS (19.67 ± 1.38 s) groups. We also detected prothrombin time (PT) and other coagulation activities of the intrinsic pathway, which were not different among the groups (Figure S2B). By combining the results of APTT, PT, and intrinsic pathway factors, we identified that AAV-shRNAs specifically inhibited FXII without causing other changes.

AAV-shRNA-Mediated Anti-thrombosis Effects on $FeCl_3$-Induced Carotid Artery Thrombosis

To evaluate the effects of shRNAs on thrombosis, we observed the blood vessels by H&E staining in $FeCl_3$-induced carotid arterial thrombosis models (Figure 3). In our study, we did not observe any thrombus in the shRNA2-treated group (Figure 3C), whereas the shRNA1 group produced remarkable obstruction similar to PBS and NC groups (Figures 3A, 3B, and 3D). Furthermore, immunofluorescence results demonstrated the deposition of fibrin in the vessels. Hence only shRNA2 could effectively inhibit carotid artery thrombosis in $FeCl_3$-induced models.

AAV-shRNA-Mediated Anti-thrombosis Effects on $FeCl_3$-Induced IVC Thrombosis

Exposure of inferior vena cava (IVC) to $FeCl_3$ would cause endothelial damage, activate platelets, and trigger the intrinsic and extrinsic pathways of coagulation, ultimately leading to thrombus formation. Based on previous studies, *PF4* and *PECAM-1*[16] were often elevated remarkably along with thrombosis. Thus, *PF4* and *PECAM-1* could contribute to estimation of clot sizes.[17] qPCR data analyses demonstrated that the *PF4* expression was low in shRNA1 (0.04 ± 0.02) and shRNA2 (0.05 ± 0.01) groups (Figure 4A). However, differences exist in *PECAM-1* (Figure 4B), wherein only shRNA2 produced a remarkable reduction (0.41 ± 0.04), and shRNA1 presented no statistical difference (0.66 ± 0.33; $p > 0.05$). By combining the results of *PF4* and *PECAM-1*, we could conclude that shRNA2 effectively restrained $FeCl_3$-induced IVC occlusion.

AAV-shRNA-Mediated Anti-thrombosis Effects on Stenosis-Induced IVC Thrombosis

To further assess the protective effect of shRNAs in thrombosis, we used partial IVC ligation for reducing the blood flow and producing minor endothelial damage that could induce IVC thrombosis. In this study, thromboembolism did not occur in shRNA2-treated mice

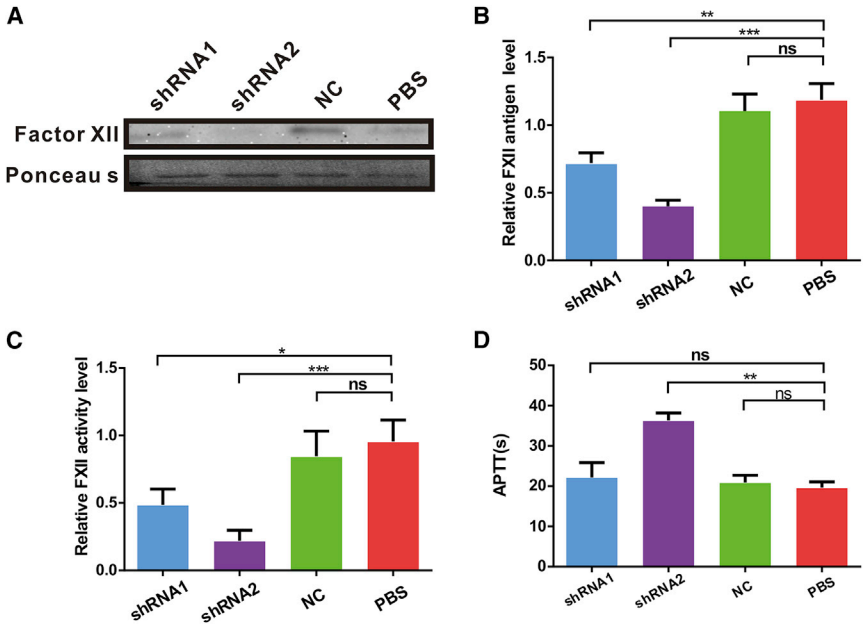

Figure 2. Comparison of Coagulation Function in Plasmas between AAV- and PBS-Treated Groups

(A) Immunoblots for plasma FXII; Ponceau staining served as the loading control. (B) Quantification of FXII relative protein levels. (C) Plasma FXII activity evaluated through clotting assays. The data were presented as percentage of pooled normal mouse plasma FXII activity. (D) *Ex vivo* APTT was quantified by clotting assays. Error bars are SD (n = 3); $^{ns}p > 0.05$, $^{*}p < 0.05$, $^{**}p < 0.01$, $^{***}p < 0.001$.

(Figure 4C). By contrast, injection of shRNA1 did not inhibit thrombosis on stenosis-induced IVC thrombosis, as well as in PBS- and NC-treated groups.

Effects of AAV-shRNA2 Treatment on Hemostasis

To determine whether shRNA2 mediated by AAV would increase hemorrhage risk, we estimated bleeding risk by bleeding time and blood loss through tail-bleeding assay (Figures 5A and 5B). The shRNA2 group exhibited no difference in blood loss and bleeding time compared with the PBS group (time: 24.2 ± 6.6 min and 38.7 ± 8.5 min for shRNA2- and PBS-treated groups, respectively). However, the mice injected with heparin showed prolonged bleeding time (>90 min) and blood loss (absorbance of lost hemoglobin, 2.69 ± 0.03).

Effects of AAV-shRNA2 Treatment on Biochemical Indicators and Histopathology

To further identify the side effects of AAV-shRNA2, we tested the plasma biochemical indicators, including alanine transaminase (ALT), creatinine (Cr), and creatine kinase (CK) (Figure S4). No difference was found between the shRNA2-treated and control groups. In addition, histological sections of the liver, brain, kidney, and heart showed that AAV-shRNA2 had no remarkable toxicity to organs (Figures 5C–5F).

DISCUSSION

Based on clinical and animal studies, FXII plays a crucial role in pathologic coagulation. Animal experiments demonstrated that depletion of FXII significantly inhibited thrombus formation and prevented the eventual occurrence of cardiovascular and cerebrovascular diseases without bleeding risk.[18] Accordingly, the proposed targeting FXII could be considered a safe anticoagulation profile. Anti-FXII drugs, such as antibodies, recombinant human albumin-infestin-4 (rHA-infestin-4), and antisense oligonucleotide, require repeated injections to induce anti-thrombosis effects or sustain only short-term effects, thereby restricting their application.

AAV-based shRNA has been widely used for gene interference. In this regard, we aim to determine whether the role of *F12*-shRNA mediated by AAV is crucial in anti-FXII and thromboembolism. In the present study, AAV8 exhibited high infection ability to liver, thereby ensuring the effective expression of shRNA to perform its function. The two shRNAs designed could reduce FXII mRNA expression and protein translation in livers. Furthermore, shRNA2 demonstrated increased inhibition capability. This conclusion could also be drawn from testing the antigen and activity of FXII in plasma. However, we found no significant difference in APTT between the shRNA1 (22.1 s) and PBS groups; meanwhile, shRNA2 could prolong the APTT (36.3 s). APTT is widely used to assess hemostasis and monitor anticoagulant therapy.[19,20] Thus, we could preliminarily estimate the antithrombotic effects. The results suggested that shRNA1 lacked sufficient ability to inhibit thrombosis.

Accordingly, we first observed whether a significant difference exists in the mouse carotid artery thrombosis to further study their function.[3] Thrombus was formed in the common carotid artery in shRNA1, PBS, and NC groups, but the opposite result was detected in shRNA2-treated mice. Hence shRNA2, and not shRNA1, possessed sufficient capability for antithrombosis.

The expression levels of *PF4* and *PECAM-1* generally increase with thrombus formatting. Thus, the mRNA levels of *PF4* and *PECAM-1* could be considered a biomarker to assess thrombogenesis. In our experiments, the *PF4* mRNA expression decreased in the shRNA-treated $FeCl_3$-induced IVC thrombosis model, whereas the expression of *PECAM-1* showed significant difference in the shRNA2 group only. We speculated that the discrepancy between *PF4* and *PECAM-1* was due to their sensibility. Although shRNA1 could not inhibit thrombosis, it can change *PF4*. We concluded that shRNA2 considerably delayed the occurrence of vein thrombus. Subsequently, the IVC thrombosis induced by stenosis was applied to evaluate anticoagulants to DVT.[21] In this study, shRNA2, but not shRNA1, presented

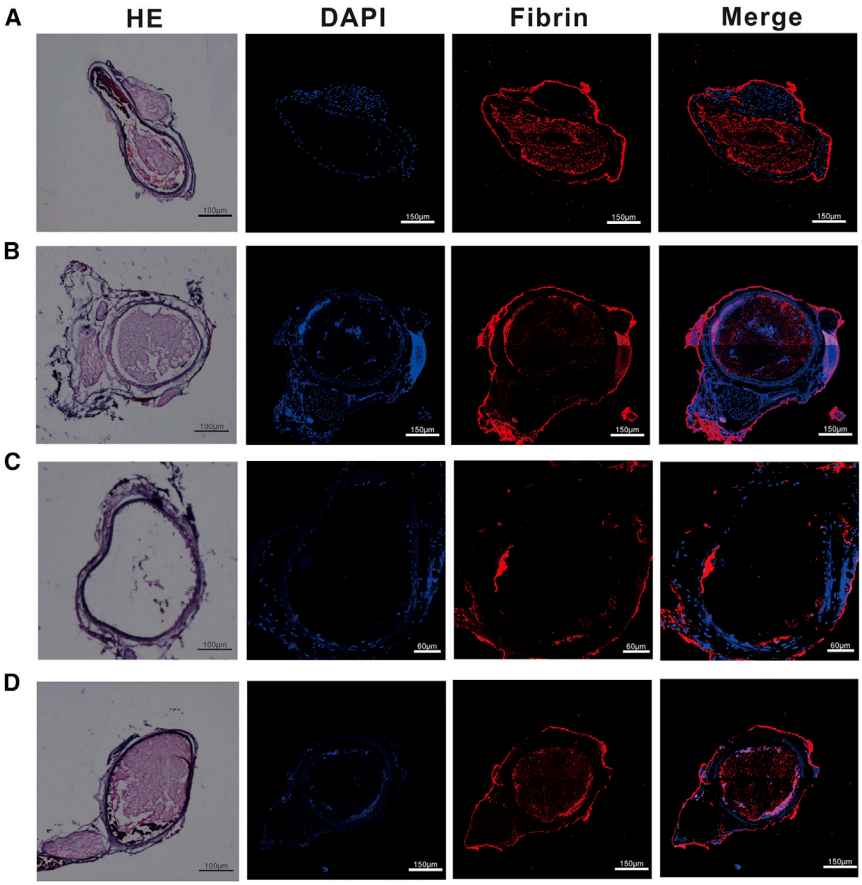

Figure 3. Effects on Arterial Thrombosis Induced by $FeCl_3$

Thrombus harvested from the carotid artery of (A) PBS-treated, (B) shRNA1-treated, (C) shRNA2-treated, and (D) nc-shRNA-treated mice. Thrombi were sectioned and subjected to immunofluorescence analysis using antibodies against fibrin or were stained with H&E.

a remarkable anti-thrombosis effect on DVT, similar to the results of previous experiments.

Several factors should be carefully considered to evaluate whether this approach would be suitable for clinical evaluation. Hence we compared bleeding time and blood loss between shRNA2 and PBS groups. As predicted, shRNA2 targeting *F12* did not increase the hemorrhage risk. Based on the analysis of histological sections and biochemical indices, AAV-based shRNA did not influence the vital signs, and thus could be suitable for application.

In summary, AAV-based shRNA can be considered an effective method for treating or preventing thromboembolic diseases.

MATERIALS AND METHODS

Design of *F12*-shRNA and AAV Vector Production

F12-shRNAs (GenBank: NM_021489.3) were designed by Invitrogen's RNAi Designer (http://rnaidesigner.thermofisher.com/rnaiexpress/). The sequences of the shRNA1 and shRNA2 are shown in Table S1. The structures of AAV8-U6-*F12*-shRNA1-CMV-ZsGreen, AAV8-U6-*F12*-shRNA2-CMV-ZsGreen, and AAV8-CMV-ZsGreen are shown in Figure S1. Vectors were constructed by HanBio Technology (Shanghai, China). The vector titers were checked by DNA dot blot method and were approximately 1.5×10^{12} viral particles per milliliter.

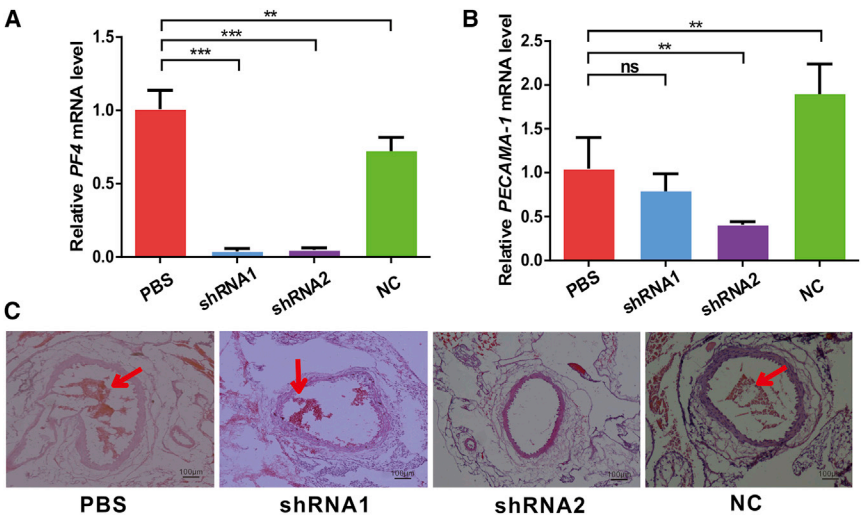

Figure 4. Effects of shRNAs on Inferior Vena Cava Thrombosis Induced by $FeCl_3$ and Stenosis

(A and B) Thrombosis was induced by 10% $FeCl_3$ solution and assessed using RT-PCR measurement of (A) *PF4* or (B) *PECAM-1* mRNA levels at the site of the IVC. (C) Thrombosis in stenosis-induced IVC among different treatment groups. IVC was obtained and stained with H&E after 24 h of vascular ligation. The red arrows indicate thrombi. Error bars are SD (n = 3); $^{ns}p > 0.05$, $^{**}p < 0.01$, $^{***}p < 0.001$.

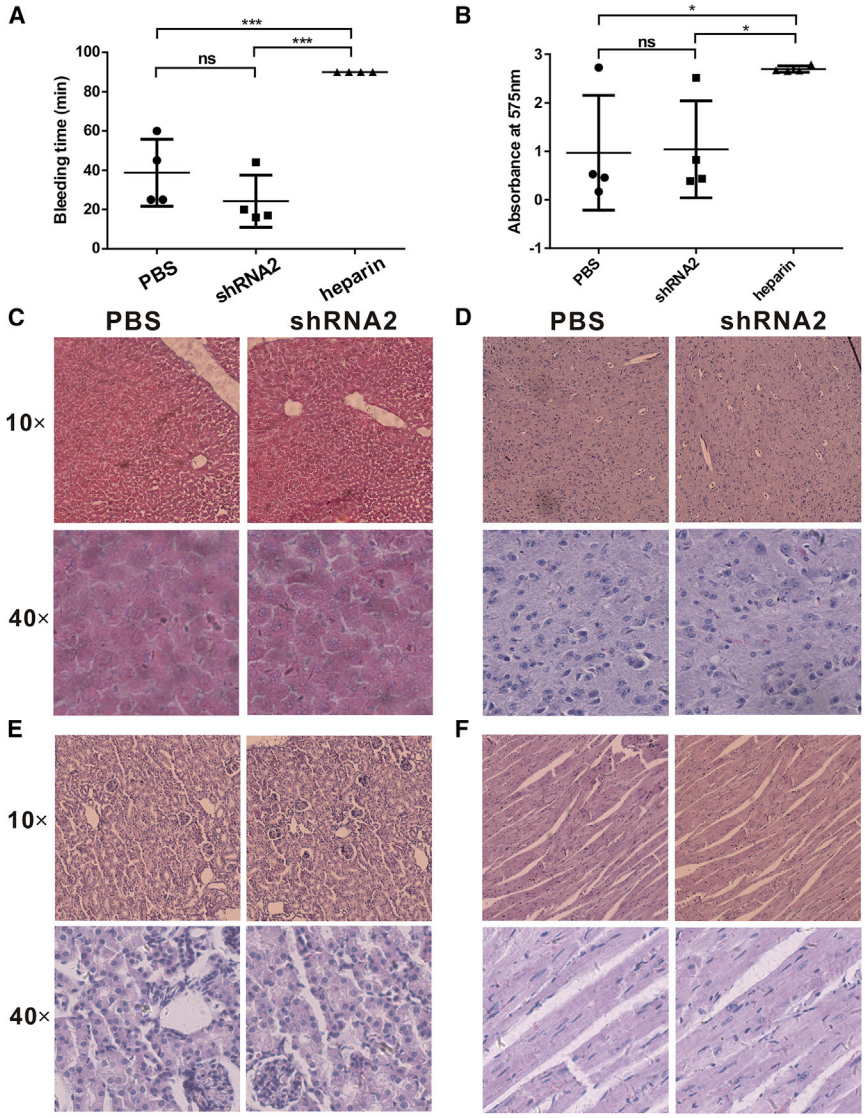

Figure 5. Effects on Hemostasis and Organic Pathology Caused by *F12*-shRNA2

(A and B) Comparison of hemostasis between PBS- and shRNA2-treated groups assessed by (A) bleeding time and (B) blood loss. (C–F) Histologic sections of (C) liver, (D) brain, (E) kidney, and (F) heart stained with H&E and observed by 10× or 40× field.

Mice and AAV Administration

Eight-week-old male C57BL/6 mice were provided by Shanghai SLAC Laboratory (Shanghai, China). The mice were housed in standard cages and handled according to institutional guidelines approved by the Animal Welfare and Use Committee of the Committee on the Ethics of Animal Experiments of the Wenzhou Medical University. The mice were injected with AAV-shRNA1, AAV-shRNA2, and AAV-nc-shRNA (0.8×10^{10} viral particles/g) by tail vein. PBS-treated mice were administered with the same volume of PBS. The mice were used in several tests with different treatments after 21 days.

Liver Fluorescence Detection

Liver sections were obtained, embedded in optimal cutting temperature compound (OCT), and frozen. Subsequently, 10-μm-thick sections were obtained by cryostat. Fluorescence was viewed in an inverted fluorescent micro6scope.

qPCR Analysis of F12 and F7 mRNA in Livers

Total mRNA was isolated from mouse livers by using TRIzol (Thermo Fisher Scientific, Waltham, MA, USA) chloroform method. cDNA was synthesized with HiScript Q RT SuperMix (Vazyme Biotech, Nanjing, China). Real-time PCR was performed on Applied Biosystem 7900 (Applied Biosystems, Foster City, CA, USA) with Sybrgreen (Vazyme Biotech, Nanjing, China). The gene and primer sequences are provided in Table S2. Experiment for qPCR was performed in triplicate, and the results were analyzed using the comparative (ΔΔCt) method.

Western Blot Analysis

Western blot was performed following the standard protocol to analyze FXII expression in the liver and plasma. GAPDH was detected with mouse anti-GAPDH antibody (cat. no. 60004-1-Ig; Proteintech Group, Chicago, IL, USA). FXII was detected with mouse anti-FXII antibody (cat. no. 66089-1-Ig; Proteintech Group, Chicago, IL, USA). Goat anti-mouse IgG (H+L) (cat. no. 925-68070; LI-COR Biosciences, Lincoln, NE, USA) was used as secondary antibody. The blots were imaged by Odyssey Imager (LI-COR Biosciences, Lincoln, NE, USA). Plasma proteins were stained by Ponceau S (cat. no. P0022; Beyotime, Shanghai, China) for internal reference.

Coagulation Function Detection

Blood was collected via carotid artery cannulas and mixed with 0.109 M sodium citrate. Plasma was prepared by centrifugation at 4,000 × *g* for 10 min to remove cellular elements. The activities of factors, APTT, and PT were detected using an automation coagulator STA-R Evolution (Stago, NJ, USA) following the standard protocol.

Arterial Thrombosis Assays

Thrombosis was induced by $FeCl_3$ through a previously reported method.[22,23] A single 1 × 2 mm strip of Whatman filter paper was soaked in a solution of 10% $FeCl_3$ and applied to the adventitial surface of the carotid artery. After 3 min, the paper was removed, and the

vessel was washed by PBS. After another 15 min, the injured vessel was embedded in OCT and cut into 10-μm sections for H&E or immunofluorescence staining. Fibrin was detected with anti-mouse fibrin IgG (cat. no. 66158-1-Ig; Proteintech Group, Chicago, IL, USA) and visualized with secondary anti-mouse Alexa Fluor 555 IgG (cat. no. A0460; Beyotime, Shanghai, China). The slides were rinsed with PBS. The coverslips were mounted with DAPI dihydrochloride (cat. no. D9542; Sigma-Aldrich, Saint Louis, MO, USA) and visualized using an LSM 880 microscope (Zeiss, Oberkochen, Germany).

Ferric Chloride-Induced IVC Thrombosis

IVC was exposed and separated from the abdomen. The process of inducing IVC thrombosis was similar to that for arterial thrombosis.[14] The injury fragment was used for mRNA extraction and detection of PF4 and PECAM-1 expression, and the process was performed following the standard protocol. The sequences of genes and primers are shown in Table S2.

Stenosis-Induced IVC Thrombosis

A 6-0 silk tie was placed behind the vessel, and a metal 4-0 suture was placed longitudinally over the IVC and tied over the top. The metal suture was removed, and two neurovascular surgical clips were applied at two separate positions below the ligation for 20 s. The bowel was replaced into the abdominal cavity, and the abdomen was closed. After 24 h, IVC was collected and fixed in 4% paraformaldehyde for H&E staining for 24 h.

Tail-Bleeding Assay

Bleeding times were determined using a previously described method.[24] The mice were anaesthetized and injected intravenously with PBS buffer. Mice in the heparin group were injected with 200 U/kg heparin. After 10 min, the mouse tails were transected 3 mm from the tip. The bleeding tail was immersed in a 15-mL test tube containing 12 mL of pre-warmed PBS. Bleeding time was recorded from the time of transection to the cessation of bleeding for 10 s. Blood loss was quantified by measuring the hemoglobin content of blood collected into PBS. After centrifugation, the pellet was lysed with lysis buffer (8.3 g/L NH4Cl, 1.0 g/L KHCO3, and 0.037 g/L EDTA). The absorbance of the sample was recorded at 575 nm. The experiment was continued until the bleeding stopped completely or at 90 min.

Biochemistry Indicator Assay and Histopathological Detection

Plasmas from shRNA2- and PBS-treated mice were collected to test ALT, Cr, and CK on VITROS@ 5600 (Ortho Clinical Diagnostics, Raritan, NJ, USA). Standard techniques for H&E staining were performed on the brains, kidneys, livers, and hearts to identify the toxic reaction on the organs.

SUPPLEMENTAL INFORMATION

Supplemental Information can be found online at https://doi.org/10.1016/j.omtn.2019.02.026.

AUTHOR CONTRIBUTIONS

M.J. conceived the idea of the study. F.L., X.Y., J.L., K.S., and C.S. performed the experiments. T.C., W.Y., S.L., and X.W. performed data analyses. M.J. wrote the manuscript. All authors have read and approved the final manuscript.

CONFLICTS OF INTEREST

The authors declare no competing interests.

ACKNOWLEDGMENTS

We would like to thank Prof. Feng Gu (School of Ophthalmology and Optometry, Eye Hospital, Wenzhou Medical University, Wenzhou, China). This work was supported by grants from the Doctoral Program of Higher Education of China (20123321120002) and the Natural Science Foundation of Zhejiang Province, China (LY13H200003).

REFERENCES

1. Puy, C., Tucker, E.I., Wong, Z.C., Gailani, D., Smith, S.A., Choi, S.H., Morrissey, J.H., Gruber, A., and McCarty, O.J. (2013). Factor XII promotes blood coagulation independent of factor XI in the presence of long-chain polyphosphates. J. Thromb. Haemost. *11*, 1341–1352.

2. Nickel, K.F., Ronquist, G., Langer, F., Labberton, L., Fuchs, T.A., Bokemeyer, C., Sauter, G., Graefen, M., Mackman, N., Stavrou, E.X., et al. (2015). The polyphosphate-factor XII pathway drives coagulation in prostate cancer-associated thrombosis. Blood *126*, 1379–1389.

3. Vu, T.T., Zhou, J., Leslie, B.A., Stafford, A.R., Fredenburgh, J.C., Ni, R., Qiao, S., Vaezzadeh, N., Jahnen-Dechent, W., Monia, B.P., et al. (2015). Arterial thrombosis is accelerated in mice deficient in histidine-rich glycoprotein. Blood *125*, 2712–2719.

4. Zamolodchikov, D., Chen, Z.L., Conti, B.A., Renné, T., and Strickland, S. (2015). Activation of the factor XII-driven contact system in Alzheimer's disease patient and mouse model plasma. Proc. Natl. Acad. Sci. USA *112*, 4068–4073.

5. van der Meijden, P.E., Munnix, I.C., Auger, J.M., Govers-Riemslag, J.W., Cosemans, J.M., Kuijpers, M.J., Spronk, H.M., Watson, S.P., Renné, T., and Heemskerk, J.W. (2009). Dual role of collagen in factor XII-dependent thrombus formation. Blood *114*, 881–890.

6. Schmaier, A.H. (2016). The contact activation and kallikrein/kinin systems: pathophysiologic and physiologic activities. J. Thromb. Haemost. *14*, 28–39.

7. Nickel, K.F., Long, A.T., Fuchs, T.A., Butler, L.M., and Renné, T. (2017). Factor XII as a Therapeutic Target in Thromboembolic and Inflammatory Diseases. Arterioscler. Thromb. Vasc. Biol. *37*, 13–20.

8. Kokoye, Y., Ivanov, I., Cheng, Q., Matafonov, A., Dickeson, S.K., Mason, S., Sexton, D.J., Renné, T., McCrae, K., Feener, E.P., and Gailani, D. (2016). A comparison of the effects of factor XII deficiency and prekallikrein deficiency on thrombus formation. Thromb. Res. *140*, 118–124.

9. Matafonov, A., Leung, P.Y., Gailani, A.E., Grach, S.L., Puy, C., Cheng, Q., Sun, M.F., McCarty, O.J., Tucker, E.I., Kataoka, H., et al. (2014). Factor XII inhibition reduces thrombus formation in a primate thrombosis model. Blood *123*, 1739–1746.

10. Zhang, H., Löwenberg, E.C., Crosby, J.R., MacLeod, A.R., Zhao, C., Gao, D., Black, C., Revenko, A.S., Meijers, J.C., Stroes, E.S., et al. (2010). Inhibition of the intrinsic coagulation pathway factor XI by antisense oligonucleotides: a novel antithrombotic strategy with lowered bleeding risk. Blood *116*, 4684–4692.

11. Yau, J.W., Liao, P., Fredenburgh, J.C., Stafford, A.R., Revenko, A.S., Monia, B.P., and Weitz, J.I. (2014). Selective depletion of factor XI or factor XII with antisense oligonucleotides attenuates catheter thrombosis in rabbits. Blood *123*, 2102–2107.

12. Woodruff, R.S., Xu, Y., Layzer, J., Wu, W., Ogletree, M.L., and Sullenger, B.A. (2013). Inhibiting the intrinsic pathway of coagulation with a factor XII-targeting RNA aptamer. J. Thromb. Haemost. *11*, 1364–1373.

13. Larsson, M., Rayzman, V., Nolte, M.W., Nickel, K.F., Björkqvist, J., Jämsä, A., Hardy, M.P., Fries, M., Schmidbauer, S., Hedenqvist, P., et al. (2014). A factor XIIa inhibitory antibody provides thromboprotection in extracorporeal circulation without increasing bleeding risk. Sci. Transl. Med. *6*, 222ra17.

14. Revenko, A.S., Gao, D., Crosby, J.R., Bhattacharjee, G., Zhao, C., May, C., Gailani, D., Monia, B.P., and MacLeod, A.R. (2011). Selective depletion of plasma prekallikrein or coagulation factor XII inhibits thrombosis in mice without increased risk of bleeding. Blood *118*, 5302–5311.

15. Burnett, J.C., Rossi, J.J., and Tiemann, K. (2011). Current progress of siRNA/shRNA therapeutics in clinical trials. Biotechnol. J. *6*, 1130–1146.

16. Falati, S., Patil, S., Gross, P.L., Stapleton, M., Merrill-Skoloff, G., Barrett, N.E., Pixton, K.L., Weiler, H., Cooley, B., Newman, D.K., et al. (2006). Platelet PECAM-1 inhibits thrombus formation in vivo. Blood *107*, 535–541.

17. Nickel, K.F., Spronk, H.M., Mutch, N.J., and Renné, T. (2013). Time-dependent degradation and tissue factor addition mask the ability of platelet polyphosphates in activating factor XII-mediated coagulation. Blood *122*, 3847–3849.

18. Hopp, S., Albert-Weissenberger, C., Mencl, S., Bieber, M., Schuhmann, M.K., Stetter, C., Nieswandt, B., Schmidt, P.M., Monoranu, C.M., Alafuzoff, I., et al. (2016). Targeting coagulation factor XII as a novel therapeutic option in brain trauma. Ann. Neurol. *79*, 970–982.

19. Sørensen, B., and Ingerslev, J. (2012). Dynamic APTT parameters: applications in thrombophilia. J. Thromb. Haemost. *10*, 244–250.

20. Trucco, M., Lehmann, C.U., Mollenkopf, N., Streiff, M.B., and Takemoto, C.M. (2015). Retrospective cohort study comparing activated partial thromboplastin time versus anti-factor Xa activity nomograms for therapeutic unfractionated heparin monitoring in pediatrics. J. Thromb. Haemost. *13*, 788–794.

21. Ponomaryov, T., Payne, H., Fabritz, L., Wagner, D.D., and Brill, A. (2017). Mast Cells Granular Contents Are Crucial for Deep Vein Thrombosis in Mice. Circ. Res. *121*, 941–950.

22. Neeves, K.B. (2015). Physiochemical artifacts in FeCl3 thrombosis models. Blood *126*, 700–701.

23. Westrick, R.J., Winn, M.E., and Eitzman, D.T. (2007). Murine models of vascular thrombosis (Eitzman series). Arterioscler. Thromb. Vasc. Biol. *27*, 2079–2093.

24. Labberton, L., Kenne, E., Long, A.T., Nickel, K.F., Di Gennaro, A., Rigg, R.A., Hernandez, J.S., Butler, L., Maas, C., Stavrou, E.X., and Renné, T. (2016). Neutralizing blood-borne polyphosphate in vivo provides safe thromboprotection. Nat. Commun. *7*, 12616.